Colloid & Polymer Science Colloid Polym Sci 272:1281–1288 (1994)

Physicochemical properties of a muramyldipeptide derivative (B30-MDP) related to membrane formation

S. Ando, H. Tsuge, and A. Miwa

Tokyo R & D Center, Daiichi Pharmaceutical Co, Ltd Tokyo, Japan

Abstract: We investigated the physicochemical properties of B30-MDP [6-O-(2-tetradecylhexadecanoyl)-N-acetyl-muramyl-L-alanyl-D-isoglutamine], a muramyldipeptide derivative having immunoadjuvant activity [1], using polarizing optical microscopy, differential scanning calorimetry (DSC), and electron spin resonance (ESR) spectroscopy. Microscopic observations showed that B30-MDP molecules form myelin figures in phosphate buffered saline (PBS). It was revealed that B30-MDP forms membranous structure because of an increase in the hydrophobicity. In the DSC measurements, the B30-MDP membrane in PBS gave no endothermic peak between 5° to 50 °C. Enthalpy change upon the phase transition from the gel to liquid crystalline state of dipalmitoylphosphatidylcholine (DPPC) membrane and its phase transition temperature decreased by the addition of B30-MDP. ESR measurements using 5 doxyl stearic acid showed that the fluidity of the B30-MDP membrane was almost comparable to that of DPPC membrane at the temperature below the phase transition temperature of DPPC, while it was lower than that of DPPC at the temperature higher than this point. The fluidity of DPPC membrane increased upon the addition of B30-MDP. These results indicate that B30-MDP forms membranous structure and that the bulky hydrophilic region of B30-MDP influences its membrane structures, thermal behavior, and membrane fluidity.

Key words: B30-MDP – dipalmitoylphosphatidylcholine – DSC – ESR – liposome

Introduction

Muramyldipeptide (MDP) is the smallest active unit of microbacteria cell wall, which has a variety of biological activities such as potentiation of antibody-mediated immune responses, and cell-mediated immune responses, induction of monocytosis, pyrogenicity, immunogenicity, and others [2].

It has thus been shown that MDP and its derivatives are useful for the development of liposomal vaccines which have higher immunogenicity [2].

New developments in the application of liposomes to vaccines have also been seen [3–5]. The great variability among liposomes in terms of structural characteristics and mode of antigen incorporation provides versatility in immunoadjuvant action and vaccine design [4]. Almeida et al. [6] produced a liposomal vaccine having antigens on the membrane surface whose shape was closely similar to that of the virus itself, and proposed the name "virosome" for these new bodies. The effectiveness of liposomal vaccines (virosomes) incorporating MDP derivatives has aroused particular interest [7]. Nerome et al. [7] reported a new type of liposomal influenza vaccine (influenza virosome) which consisted of hemagglutinin-neuraminidase (HANA) antigen, cholesterol, and an MDP derivative [6-O-(2-tetradecylhexadecanoyl)-N-acetyl-muramyl-L-alanyl-D-isoglutamine: B30-MDP]. B30-MDP was synthesized as a MDP analog which has less toxicity and is more potent than the immunoadjuvant

activity of MDP [1]. While Nerome et al. (1990) suggested membrane formation of B30-MDP, physicochemical properties of B30-MDP in membrane formation have not been described. It is of importance for a design of liposomal vaccine to know basic characteristics of a lipid which has immunoadjuvant activity.

Comparing to dipalmitoylphosphatidylcholine, in the present study we investigated the physicochemical properties of B30-MDP in membrane formation, such as its self-organization of vesicles, thermotropic behavior, and alkyl-chain flexibility, by using polarizing optical microscopy, differential scanning calorimetry (DSC), and electron spin resonance (ESR) spectroscopy.

Materials and Methods

Chemicals

Muramyldipeptide derivative, [6-O-(2-tetradecylhexadecanoyl)-N-acetyl-muramyl-L-alanyl-D-isoglutamine] (B30-MDP), synthesized by Daiichi Pharmaceutical Co., Ltd. (Tokyo, Japan), was used in the present study. The chemical structure of B30-MDP is shown in Fig. 1. Dipalmitoylphosphatidylcholine (DPPC) (99%, Nichiyu Liposome Co., Ltd., Tokyo, Japan) was used without further purification. The spin probes 5-doxyl-stearic acid (5 NS) and 16-doxyl-stearic acid (16 NS) were obtained from Aldrich Chemical Co., Ltd. (Wl., U. S. A.)

Polarizing optical microscopic observation

Polarizing optical microscopy of myelin figures of B30-MDP was performed as follows. About 1 mg of a lump of B30-MDP was placed on a glass slide. About 50 μL of solvent (solvents were distilled water, 0.05 M phosphate buffer (PB), pH 7.4, and phosphate buffered saline (PBS), pH 7.4) was then added to the lump from all sides. A cover slip was put on the lump over spacers of about 100 μm thickness and pressed down to prevent the lump from distorting. Drops of solvent were added to the lump edge, then a figure of the lump was photographed after storage for 24 h at 20 °C.

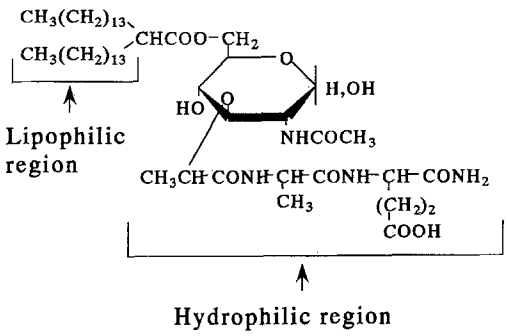

Fig. 1. Chemical structure of B30-MDP

Differential scanning calorimetry (DSC)

Samples for DSC measurement were prepared by drying of DPPC, B30-MDP, and a DPPC/B30-MDP mixture in chloroform under dry nitrogen, then placing them under high vacuum for at least 8 h. The lipid-films were rehydrated with PBS (pH 7.4) at above 50 °C and vortexed several times to produce multilamellae vesicles (MLV). Twenty μL of the MLV containing about 2 mg of lipids was transferred into an aluminum sample pan. After the pan was sealed, the sample was kept for 1 h at 50 °C. All measurements were carried out with a Du Pont 910 DSC at a scanning rate of 2.0 °C/min while heating the pan from 5° to 50 °C. In this experiment, B30-MDP concentration was calculated from the following equation:

$$\text{B30-MDP (\%)} = (\text{molarity of B30-MDP}/(\text{molarity of DPPC} + \text{molarity of B30-MDP})) \times 100 \quad (1)$$

Electron spin resonance (ESR)

Spin-labeled vesicles were prepared as follows. B30-MDP, DPPC, and the spin probes were dissolved separately in chloroform. When these solutions were mixed in a 20- mL round bottomed flask, the content of spin probes was approximately 1 mol% of total lipids, and that of B30-MDP ranged from 0 to 40 mol%. B30-MDP concentration was calculated from Eq. (1). This solution was rotary-evaporated to dryness under vacuum at room temperature. Then, PBS at a temperature above 50 °C was added to the lipid films in a round bottomed flask and sonicated to disperse the vesicles with a probe-type sonicater

(Ohtake Works) for 3 min at 30 watts. PBS was then added to bring the lipid concentration to 50 μmol/mL.

Fifty μL of the dispersed vesicles was drawn into a disposable micropipette (Drummond Scientific Co.) used as a sample tube. The pipette was sealed at one end with a Hemat sealer, and maintained in a fixed position in the ESR cavity. ESR spectra were recorded at X-band, 3268 G magnetic field, 100 G scanning range, 100-kHz field modulation, 0.8-gauss modulation width and 8 mW microwave power with a JEOL JES-FE2XG spectrometer equipped with a variable temperature control unit. The outer hyperfine splitting constant, A_{max}, was obtained from the separation ($2A_{max}$) between the low-field maximum and the high-field minimum peaks in experiments using 5 NS as reported by McConnell et al. [8]. When 16 NS was used as a spin probe, the ratio of the low-field resonance line to that of the center-field [$h(+)/h(0)$] was used as the experimental semiquantative measure of hydrocarbon chain flexibility [9].

Results and discussion

Polarizing optical microscopic observation

It is well known that hydrated natural phospholipids form elongated tubular structures, called myelin figures [10, 11]. We examined myelin figures grown from B30-MDP lumps with several solvents using a polarizing optical microscope.

Myelin figures of the hydrated B30-MDP lumps are shown in Fig. 2. B30-MDP hydrated with water which indicated an isotropic phase did not form myelin figures (Fig. 2a). Myelin figures could be observed in PB, but their shape was unstable (Fig. 2b). In contrast, myelin figures from B30-MDP in PBS were distinctly observed (Fig. 2c).

Generally, the myelin figure is composed of a multilamellae of lipid bilayers concentrically stacked with a considerable amount of medium inside the tube, and is formed spontaneously at the gel-to-liquid crystalline phase transition temperature [10]. Myelin figure formation provides important evidence for the self-organizational ability of a membrane. Kunitake et al. [12, 13] have reported the formation of bilayer structures from many kinds of simple synthesized amphipatic compounds. Accordingly, the results of these observations indicate that B30-MDP, like

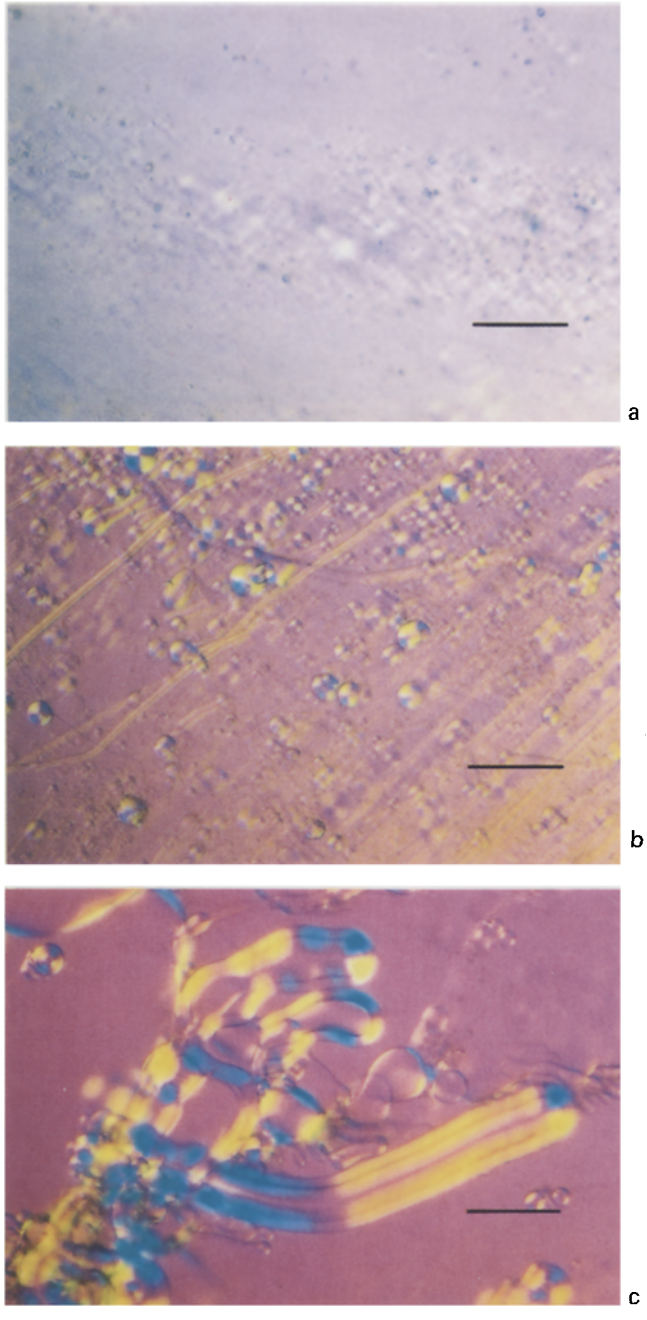

Fig. 2. Polarizing optical micrographs of myelin figures of B30-MDP in a) water, b) PB, and c) PBS taken with crossed-Nichols. Bar = 100 μm

phospholipids, is able to form membranes in PBS and that the phase of B30-MDP membrane at 20 °C was a liquid crystal.

It is likely that the membrane-forming ability of B30-MDP is closely related to salt concentration in the solvent. The carboxylic group in the bulky hydrophilic region of B30-MDP (Fig. 1) dissociates to the ion form in PB (pH 7.4) or in water. However, it is estimated that the hydrophobicity of B30-MDP increases with increasing salt concentrations in the buffer, the so-called salting-out effect. We concluded that the molecular orientation and packing of B30-MDP are enhanced by the increase in hydrophobicity caused by the salting-out, and that myelin figures of B30-MDP formed in PBS are particularly stable. It is considered that B30-MDP, which has immunoadjuvant activity and an ability of membrane formation, is useful for a design of liposomal vaccine.

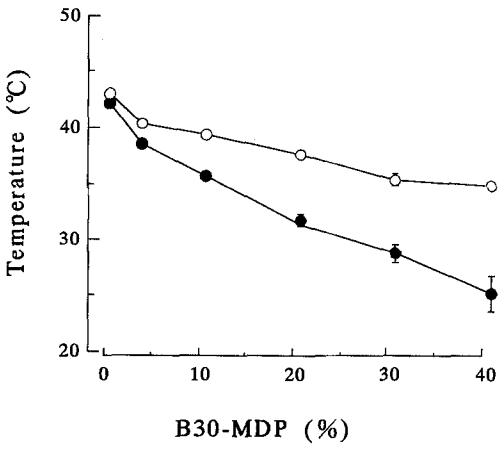

Fig. 3. Effect of B30-MDP on the gel-to-liquid crystalline phase transition temperature of DPPC membrane measured by DSC. *Te*.o; extrapolated onset temperature (●) and *Tp*; peak point temperature (○). Vertical bars denote S. D. for a series of three separate determinations

DSC measurements

DSC measurements were performed to identify the effects of B30-MDP against the temperature and enthalpy in the phase transition from the gel to liquid crystalline state of DPPC membrane in PBS.

Changes in phase transition temperature: The endothermic peak indicating gel-to-liquid crystalline phase transition of DPPC membranes was about 42 °C. The phase transition peaks broadened with increasing B30-MDP concentration in the membranes, rendering identification of the endothermic peak difficult. The effect of B30-MDP on the separation of the extrapolated onset (*Te*.o) and peak point (*Tp*) temperatures of gel-to-liquid crystalline phase transition of DPPC membrane is shown in Fig. 3. Both *Te*.o and *Tp* were decreased with increasing B30-MDP concentrations; in particular, a pronounced decrease in *Te*.o was seen, which reflected peak broadening. At concentrations of B30-MDP in DPPC membrane above 40%, no endothermic peak for phase transition could be identified.

These results are similar to those obtained with binary membranes of DPPC with other phospholipids having a lower *Tp* than DPPC [14]. The mixture state of binary lipid membranes, such as ideal mixing or phase separation, is confirmed by a phase diagram. The change of main transition peak width of DPPC/B30-MDP membrane is shown in Fig. 3. Mabrey et al. [14] reported the thermotropic behavior of binary phosphatidylcholines systems whose chain lengths differed by 2,4 or 6 carbons. In their studies, two lipids which differed by two carbons in the lengths of their acyl chains only (dimyristoylphoshpatidylcholine(DMPC)/DPPC) appeared to form a nearly ideal mixture, which was confirmed by the agreement of theoretical with experimental phase diagrams. Deviation from ideality was found in a system in which the acyl chain lengths differed by four carbons (DMPC/distearoylphoshpatidylcholine (DSPC)), wherein significant phase separations occurred. When the lengths differed by six carbons (dilauroylphoshpatidylcholine/DSPC), the system was so far from ideal that monotectic behavior was observed. We concluded from these results that the gel-to-liquid crystalline phase transition temperature of B30-MDP membrane in the present study was lower than that of DPPC. It was shown that the mixture state of B30-MDP/DPPC membrane did not form an ideal mixture, because the chemical structure of the bulky hydrophobic region of B30-MDP differed from that of DPPC and the transition peak was broadened, finally disappearing with increasing B30-MDP.

Enthalpy changes in phase transition: Figure 4 shows the effect of B30-MDP on the gel-to-liquid crystalline phase transition of DPPC membrane as the enthalpy changes calculated from DSC curves. It was estimated that the enthalpy changes decreased linearly with increasing B30-MDP concentration, reaching zero at about 70 mol%. An unchanged curve was obtained in the 5° to 50 °C range in DSC measurement of B30-MDP membrane (data not shown). The results of the DSC studies and the fact that myelin figures of B30-MDP formed at 20 °C in PBS suggested that the phase of B30-MDP at a temperature above 5 °C is a liquid crystal phase. These results also indicated that the B30-MDP/DPPC membrane did not form an ideal mixture, because the transition enthalpy was extrapolated to zero at a B30-MDP membrane concentration of 70 mol%. This implies that the gel-to-liquid crystalline phase transition peak of B30-MDP exists at a temperature below 5 °C, and that the gel-to-liquid crystalline phase enthalpy of B30-MDP in DPPC membrane increases with increasing B30-MDP concentration. We concluded that the interaction of mutual hydrophobic regions in DPPC membrane was inhibited by the addition of B30-MDP in liquid crystalline phase at a temperature above 5 °C [15–17].

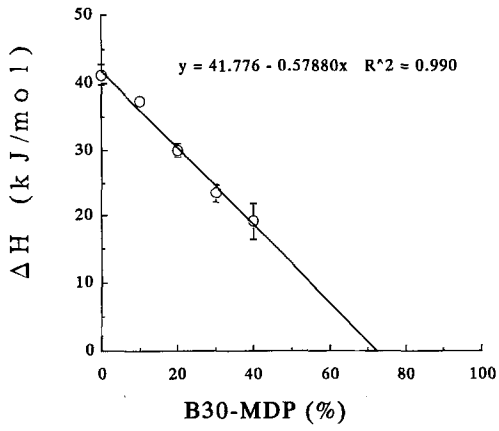

Fig. 4. Effect of B30-MDP on the gel-to-liquid crystalline phase transition enthalpy of DPPC membrane measured by DSC. Vertical bars denote S. D. for a series of three separate determinations

ESR measurements

ESR measurements were performed to determine the fluidity of B30-MDP membrane, DPPC membrane, and binary B30-MDP/DPPC membrane.

Single component membrane: The ESR spectral parameters of 5 NS in DPPC and B30-MDP membranes at various temperatures are shown in Fig. 5. The fluidity of DPPC and B30-MDP membranes was measured with 5 NS, in which the nitroxide monitoring group is positioned near the headgroup region of the lipid bilayer. The fluidity of DPPC membrane measured with 5 NS was markedly increased at 42 °C, that is, the change in A_{max} value indicated the gel-to-liquid crystalline phase transition [18]. In contrast, the changes in B30-MDP membrane A_{max} value indicated that phase transition was not observed between 20° to 50 °C. As shown in Fig. 5, the fluidity of B30-MDP membrane was almost the same as that of

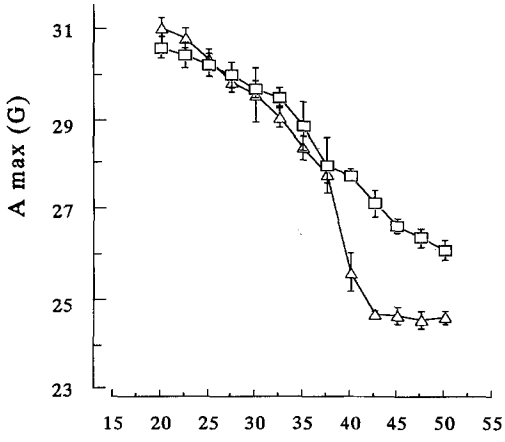

Fig. 5. The membrane fluidity expressed by the peak width (A_{max}) of the ESR spectra for 5 NS at various temperatures. △, DPPC, and □, B30-MDP. Vertical bars denote S. D. for a series of three separate determinations

DPPC membrane below 42 °C and lower than that of DPPC membrane above 42 °C. These results suggested that overall, the fluidity of B30-MDP membrane as measured with 5 NS was lower than that of DPPC membrane.

ESR spectral parameters of 16 NS in DPPC and B30-MDP membranes at various temperatures are

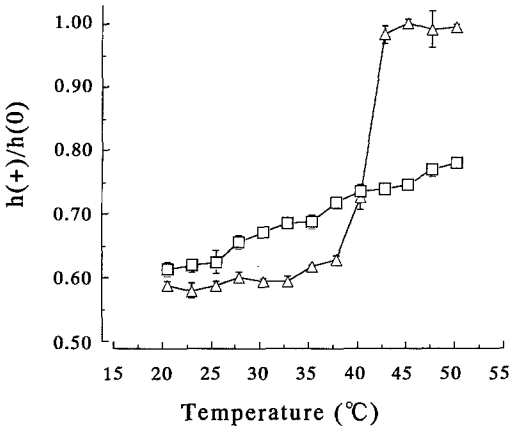

Fig. 6. Membrane fluidity expressed by the peak height ratio ($h(+)/h(0)$) of the ESR spectra for 16 NS at various temperatures. △, DPPC membrane, and □, B30-MDP membrane. Vertical bars denote S. D. for a series of three separate determinations

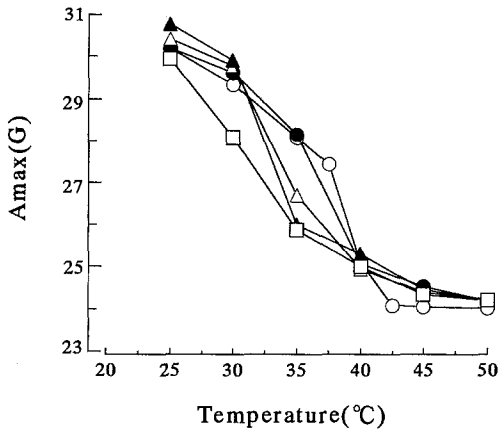

Fig. 7. Effect of B30-MDP on the peak width (A_{max}) of the ESR spectra for 5 NS in membranes at various temperatures. Various B30-MDP concentrations of 0% (○), 10% (●), 20% (△), 30% (▲), and 40% (□). Each point represents the mean of three experiments

shown in Fig. 6. The fluidity of these membranes was measured with 16 NS, in which the nitroxide monitoring group is positioned deep within the hydrophobic region of the lipid bilayer. The fluidity of DPPC measured with 16 NS was markedly increased at about 42 °C. This finding accorded with that using 5 NS and the results of the DSC study. As shown in Fig. 6, the fluidity of B30-MDP membrane measured with 16 NS was higher than that of the DPPC membrane below 42 °C and lower than that of DPPC membrane above 42 °C. The changes in $h(+)/h(0)$ value in B30-MDP membrane indicated that phase transition was not observed between 20° to 50 °C. These results (Figs. 5 and 6) corresponded with those of the DSC study, in which no transition peak of B30-MDP membrane could be identified.

Although polarizing optical microscopy and DSC showed that the phase of B30-MDP membrane above 20 °C was a liquid crystal phase, the fluidity of B30-MDP membrane at a temperature below 42 °C indicated a low value closely similar to the gel phase of DPPC membrane, particularly when measured with 5 NS. These results suggest that a stable structure of mutual hydrophilic regions of B30-MDPs is formed. We concluded that the fluidity of the hydrophobic region of B30-MDP is decreased by the stable structure of hydrophilic region.

Binary membrane: ESR spectral parameters of 5 NS in DPPC membranes with B30-MDP at various temperatures are shown in Fig. 7. The fluidity of binary mixtured membranes measured with 5 NS below 42 °C was clearly influenced by increasing B30-MDP concentration, and the onset temperatures, as reflected by the starting-point of obvious fluidity increase, were decreased. Further, the fluidity difference between the gel phase and liquid crystalline phase became ambiguous as B30-MDP concentration increased.

The ESR spectral parameters of 16 NS in DPPC membranes with B30-MDP at various temperatures are shown in Fig. 8. The fluidity of binary membranes measured with 16 NS were clearly influenced by increasing B30-MDP concentration. Both onset temperature and terminal temperature were decreased. The fluidity difference between the gel and liquid crystalline phases gradually decreased as B30-MDP concentration increased. Fluidity changes of binary mixtured membranes measured with 5 NS were almost the same as those with 16 NS.

To confirm the correlation between the results of the ESR measurement with 16 NS and those of the DSC study, we compared the onset temperatures of the DSC curves and ESR spectra [19] (Fig. 9). Additionally, peak point temperatures of DSC curves and mid-point temperatures of ESR spectra were also compared. Results demonstrated that the ESR and DSC studies were well correlated.

By the addition of B30-MDP to DPPC membranes, transition enthalpy and temperature

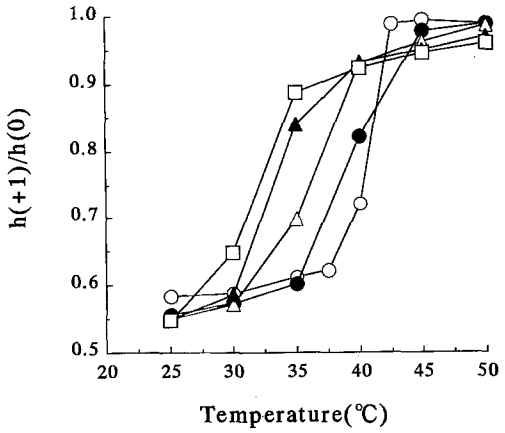

Fig. 8. Effect of B30-MDP on the peak height ratio ($h(+)/h(0)$) of the ESR spectra for 16 NS in membranes at various temperatures. Various B30-MDP concentrations of 0% (○), 10% (●), 20% (△), 30% (▲), and 40% (□). Each point represents the mean of three separate experiments

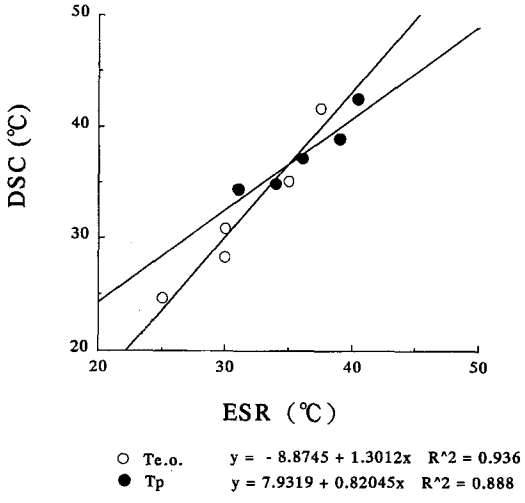

Fig. 9. Correlation between results of DSC and ESR measured with 16 NS. ○, comparison of onset temperature ●, comparison of peak point temperature obtained from DSC curves and mid-point temperature obtained from ESR spectra

decreased as fluidity of the mixed membranes increased. Our results indicated that membranes consisting of both DPPC and B30-MDP become a less stable structure than those consisting of either B30-MDP or DPPC alone.

The molecular orientation and packing of B30-MDP, however, were improved by the increase in hydrophobicity caused by salting-out; stable myelin figures of B30-MDP were formed in the high salt concentration buffer solutions (PBS). The ESR study showed that the fluidity of B30-MDP membrane decreased because of the structural effect of the hydrophilic region of B30-MDP.

We concluded that the dissociative state and the structural effect of the hydrophilic region of B30-MDP influence its membrane formation, thermal behavior and membrane fluidity.

For the use of B30-MDP as a virosome, it is important to confirm the physicochemical stability of the membrane, which will be affected by the addition of the phospholipids and the antigens.

Acknowledgment

The authors would like to thank Drs. Y. Osada, T. Onodera and K. Ito (Daiichi Pharmaceutical Co., Ltd.) for their helpful advice and discussion.

This work was supported by a grant from Japan Health Science Foundation.

References

1. Kusumoto S, Inage M, Shiba T, Azuma I, Yamamura Y (1978) Tetrahedron Lett 49:4899–4902
2. Adam A, Lederer E (1984) Med Res Rev 4:111–152
3. Oxford JS, Hockley DT, Heath TD, Patterson S (1981) J Gen Virol 52:329–343
4. Gregoriadis G (1990) Immunology Today 11:89–97
5. Reddy R, Nair S, Brynestad K, Rouse BT (1992) Semin Immunol 4:91–96
6. Almeida JD, Brand CM, Edwards DC, Heath TD (1975) Lancet 8:899–901
7. Nerome K, Toshioka Y, Ishida M, Oka T, Kataoka T, Inoue A, Oya A (1990) Vaccine 8:503–509
8. McConnell HM, Wright KL, McFarland BG (1972) Biochem Biophys Res Commun 47:273–281
9. Humphries GMK (1980) In: Gregoriadis G, Allison AC (eds) Liposomes in Biological Systems, John Wiley & Sons Inc Chichester pp. 345–376
10. Kelker H (1973) Mol Cryst Liquid Cryst 21–48
11. Chapmann D, Fluck DJ (1966) J Cell Biol 30:1–11
12. Kunitake T, Kimizuka N, Higashi N, Nakashima N (1984) J Am Chem Soc 106:1978–1983
13. Kunitake T, Okahata Y (1977) J Am Chem Soc 99:3860–3861
14. Mabrey S, Sturtevant JM (1976) Proc Natl Acad Sci USA 73:3862–3866
15. Kodama M (1990) Yukagaku 39:530–537
16. Kodama M, Tsuchiya S, Nakayama K, Takaichi Y, Sakiyama M, Akiyoshi K, Tanaka K, Sunamoto J (1990) Thermochimica Acta 163:81–88
17. Wiener JR, Wagner RR, Freire E (1983) Biochemistry 22:6117–6123

18. Shimshick EJ, McConnell HM (1973) Biochem Biophys Res Commun 53:446–451
19. Hubbell WL, McConnell HM (1971) J Am Chem Soc 93:314–326

Received September 24, 1993;
accepted February 22, 1994

Authors' address:

Mr. Shuichi Ando
Tokyo R & D Center
Daiichi Pharmaceutical Co., Ltd.
16–13, Kita-kasai 1-chome, Edogawa-ku Tokyo 134
Japan.